Charge transfer and electronic transitions in polycrystalline $BiFeO_3$

B. Ramachandran,[1] A. Dixit,[2] R. Naik,[2] G. Lawes,[2] and M. S. Ramachandra Rao[1,*]
[1]*Department of Physics, Nano Functional Materials Technology Centre and Materials Science Research Centre, Indian Institute of Technology Madras, Chennai, Tamil Nadu 600036, India*
[2]*Department of Physics and Astronomy, Wayne State University, Detroit, Michigan 48201, USA*
(Received 14 March 2010; revised manuscript received 26 May 2010; published 16 July 2010)

We report on the electronic energy-level diagram of polycrystalline $BiFeO_3$ using the elemental, optical, and current-density-electric field (*J-E*) characteristics. The elemental, electronic composition, and valence-band structure of $BiFeO_3$ ceramics were studied using x-ray photoelectron spectroscopy. The diffuse reflectance spectrum of a mixture of $BiFeO_3$ and $BaSO_4$, used as a standard, was recorded to test the Kubelka-Munk model. From the graph of the Kubelka-Munk function versus wavelength, two charge-transfer bands and two doubly degenerated *d-d* transitions ($^6A_{1g} \rightarrow {}^4T_{2g}$ and $^6A_{1g} \rightarrow {}^4T_{1g}$) were observed in polycrystalline $BiFeO_3$. The *J-E* curves measured on the $BiFeO_3$ ceramics showed space-charge-limited conduction mechanism.

DOI: 10.1103/PhysRevB.82.012102 PACS number(s): 71.35.Cc, 75.50.Ee, 72.80.Sk

Multiferroic materials exhibit the coexistence of two or more order parameters.[1–3] The possible complex interactions among these order parameters make such materials very promising candidates for the development of new spintronic and optoelectronic devices. However, in many materials, this cross coupling among magnetic, electric, and structural order parameters has been found to be small, seriously limiting the device prospects of these systems. In order to optimize the magnetoelectric coupling in these multiferroic materials, it is crucial to first develop a complete understanding of the electronic structure in these systems. The focus of this investigation is the promising multiferroic, $BiFeO_3$, which exhibits a number of intriguing properties, but which is not typically studied in depth in bulk polycrystalline samples.

The interest in $BiFeO_3$ arises due to the fact that it is one of only two or three single-phase multiferroic material system above room temperature identified in the literature, which makes it potentially the most relevant material for device applications. It is a commensurate ferroelectric and incommensurate antiferromagnetic system at room temperature. The multiferroic and optoelectronic properties of $BiFeO_3$ make it a potential candidate for next-generation ferroelectric random access memories, magnetic sensors,[1] and photovoltaics.[4] However, despite the interest in $BiFeO_3$, several fundamental properties for this system remain controversial; most significantly there is still a debate on the nature and value of the band gap. Theoretical studies along with some experimental investigations, report direct band-gap values ranging from 2.5 to 2.8 eV.[4–8] However, recent optical studies, including absorption measurements and cathode-luminescence spectroscopy, show evidence for a direct optical band gap near 2.5 eV.[9] An indirect band gap of ~1.84 eV has also been reported for $BiFeO_3$,[10] based on spectroscopic ellipsometry studies. However, recent theoretical studies of the charge-transfer (CT) transitions together with spectroscopic measurements of the dielectric function of a $BiFeO_3$ single crystal and other related Fe^{3+} iron oxides[9] show a defect free intrinsic band gap of ~3.0 eV, superimposed on a weak absorption band at ~2.5 eV. Optical spectroscopy is a widely used probe of electronic structure in solids and when charge and spin degrees of freedom are strongly coupled, it is also sensitive to magnetic excitations and spin ordering transitions.[11,12] A clear understanding of the in-gap states is necessary for understanding the conductivity mechanisms and intrinsic leakage currents in multiferroics. A better understanding of the mechanisms governing the optical response in $BiFeO_3$ can enable researchers to engineer the band gap and conductivity to enhance the photoferroelectric properties.[4]

We synthesized single-phase polycrystalline $BiFeO_3$ ceramics using a sol-gel approach. X-ray diffraction and scanning electron microscopy were carried out for structural analysis. We also performed structural refinement to estimate the lattice parameters and phase purity of the material. The magnetic and magnetocaloric properties of these $BiFeO_3$ ceramics were also investigated and have been published in a recent report.[13] In order to understand the fundamental electronic properties of polycrystalline $BiFeO_3$, we report on the electronic excitations and band structure of $BiFeO_3$ ceramics investigated using x-ray photoelectron spectroscopy (XPS), diffuse reflectance spectroscopy (DRS), and current density-electric field (*J-E*) characteristics.

Elemental analysis and valance-band studies of $BiFeO_3$ ceramics were carried out using an XPS system from Perkins Elmer. Diffuse reflectance spectra and current-density-electric field (*J-E*) characterization were recorded using an Ocean Optics spectrometer (USB2000, USA) and a Precision Premier II ferroelectric loop tracer (Radiant technologies, USA), respectively. We used DRS to investigate the optical properties of the sample using a dilution technique that eliminates the regular part of the reemitted radiation. This was done by diluting a 10 wt % of $BiFeO_3$ sample by mixing it homogeneously with an inactive, nonabsorbing standard $BaSO_4$ powder and pelletizing the composite with a pressure ~80 kg/cm^3 using hydraulic press to record diffuse reflectance spectrum. The spectrum was recorded over the full spectral range from 200 to 900 nm. This method facilitates an experimental comparison with the Kubelka-Munk (K-M) model.[14] For the *J-E* characteristic study, the sintered pellet was polished on both sides and then cleaned thoroughly with acetone. The polished $BiFeO_3$ pellet was subsequently annealed at 673 K for 6 h to remove the residual surface stress left from polishing and then silver paste

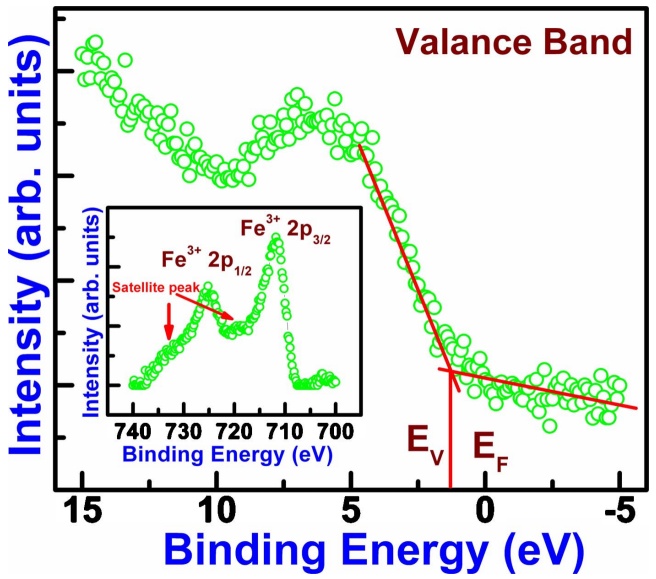

FIG. 1. (Color online) X-ray photoelectron spectra of valence band and Fe element (inset) of polycrystalline $BiFeO_3$ ceramics.

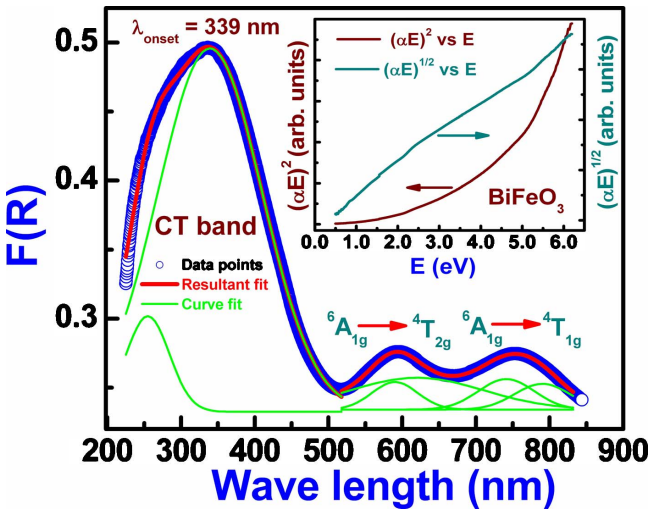

FIG. 2. (Color online) Kubelka-Munk function, $F(R)$ vs wavelength of polycrystalline $BiFeO_3$ by dilution method. CT and double degenerated d-d transitions of Fe^{3+} ion-$^6A_{1g} \rightarrow {}^4T_{2g}$ and $^6A_{1g} \rightarrow {}^4T_{1g}$. Inset shows the plots of $(\alpha E)^2$ vs E and $(\alpha E)^{1/2}$ vs E of polycrystalline $BiFeO_3$ sample.

was applied on both sides of $BiFeO_3$ pellet in parallel plat geometry to measure the J-E characteristics.

XPS measurements of the electron binding energies correspond to Bi, Fe, and O, confirming the phase purity of the compound. Figure 1 shows the binding energy of the valence band, determined using XPS measurements. From these data, we estimate the separation between the valance-band energy (E_V) and the Fermi energy (E_F) to be ~1.25 eV. The inset of Fig. 1 shows the XPS spectrum expanded around the Fe peaks, in the range from 700 to 740 eV. The 3/2 and 1/2 spin-orbit doublet components of the Fe $2p$ photoelectron were found to be located at 710.3 eV and 724.5 eV, respectively. These XPS results confirm the single-phase formation of $BiFeO_3$ ceramic with iron being present in the 3+ valence state. We do not find evidence for any Fe^{2+} impurities in the sample, which have previously been proposed as a source of enhanced electrical conductivity in other $BiFeO_3$ samples.[15]

The K-M function, $F(R)=(1-R)^2/2R$, which correlates reflectance is plotted as a function of wavelength (Fig. 2) by using the measured diffuse reflectance (R) of $BiFeO_3$ sample.[14] By extrapolating $F(R)^{1/2}$ to zero, we estimate the direct band gap of $BiFeO_3$ at 300 K to be ~2.5 eV. Previous electronic-structure investigations have already established the strongly hybridized nature of the valence bands[16,17] and although the mixing of Fe^{3+} d levels with O p and Bi s states affects the chemical bonding, it does not change the symmetry of the crystal-field-derived bands. Therefore, in the interest of clarity, the electronic structure will be discussed using traditional ligand field terminology but with the understanding that these states are, in reality, strongly hybridized. In particular, by considering the C_{3v} local symmetry of Fe^{3+} ions in $BiFeO_3$ and using the correlation group and subgroup analysis of the symmetry breaking from O_h to C_{3v}, up to six d to d excitations are expected for $Fe^{3+}(3d^5)$ ions between 0 and 3 eV. Note that the triply degenerate $^4T_{1g}$ and $^4T_{2g}$ electronic levels split into two crystal-field levels having A and E character due to a reduction in symmetry. The near band-gap charge-transfer bands (or states) and d-d transitions of Fe^{3+} ions were calculated from the DRS spectrum through a deconvolution of these data. Two strong transitions observed near 3.6 and 4.8 eV are assigned as CT excitations.[16,17] Two broad reflectance bands between 1 and 2.5 eV predicted (but spin forbidden) to be on-site d-d crystal-field excitations of Fe^{3+} ions in this energy range, can be resolved as four different linear oscillator components having imaginary components of susceptibility $\chi_{ij}^{(1)}$.[18] The two doubly degenerate d-d excitation ($^6A_{1g} \rightarrow {}^4T_{2g}$ and $^6A_{1g} \rightarrow {}^4T_{1g}$) energies of Fe^{3+} ions in $BiFeO_3$ were found to fall at 1.6, 1.7, 2.0, and 2.1 eV which are close to the reported values of $BiFeO_3$ single crystal and thin films.[19] We also carried out the absorption studies by measuring absorption coefficient (α) as a function of energy of $BiFeO_3$ sample using UV-visible spectroscopy (inset of Fig. 2). By plotting the dependence of $(\alpha E)^2$ and $(\alpha E)^{1/2}$ on E,[8,10] the values of direct and indirect band gap can be determined by extrapolating the linear portions of these plots to $(\alpha E)^2$ equal to zero and $(\alpha E)^{1/2}$ equal to zero, respectively. It is found that these data are consistent with a direct band gap,[9] however, it is not possible draw conclusions from the above study as the possibility of an indirect transition from a flat valence band still remains an issue.[16]

Figure 3 shows a typical logarithmic plot of the current density (J) versus the applied electric field (E). The slope of this curve in the low-field range (or near origin) is close to 1.27 which is roughly consistent with ohmic conduction. Below an applied voltage of 1.92 kV which corresponds to the electric field strength of 25.60 kV/cm, the slope of the curve is smaller than 2, suggesting a trap free conduction mechanism. At higher applied voltages (>1.92 kV), the slope of the logarithmic plot of J-E increases, in agreement with space-charge-limited current conduction. The conduction current in the space-charge-limited current conduction can be expressed as[19]

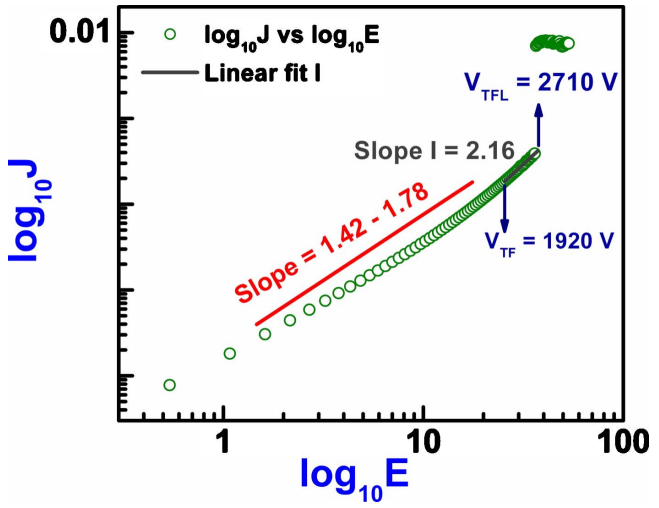

FIG. 3. (Color online) A typical logarithmic plot of current density-electric field (J-E) characteristics of polycrystalline $BiFeO_3$ ceramics.

$$J = \frac{9}{8}\varepsilon_r\varepsilon_0\theta\mu\frac{V^n}{d^3},$$

where V is the applied field, d is the sample thickness, ε_0 is the permittivity of free space, ε_r is the dielectric constant, μ is the mobility, θ is the ratio of free electrons to trapped electrons, and n is the power factor. Assuming a single discrete shallow trap level in $BiFeO_3$, the trapped electron density (N_t) can be calculated from the trap-filled limit voltage (V_{TFL}) using[20]

$$N_t = \frac{9}{8q}\varepsilon_r\varepsilon_0\frac{V_{TFL}}{d^2},$$

where q is the charge. Experimentally, V_{TFL}, ε_r, and θ obtained from Fig. 3 are 2710 V, 5.6, and 2×10^{-3}, respectively. The calculated value of N_t at 300 K is 2×10^{18} cm^{-3}. The trap-level energy E_t can be calculated relative to the conduction-band energy E_c using,[20]

$$\theta = \frac{N_c\exp[(E_t - E_c)/kT]}{gN_t},$$

where N_c is the effective density of states in the conduction band and g is the degeneracy factor ($\sim$2). For our $BiFeO_3$ samples, N_c is assumed to be 10^{21} cm^{-3}. These estimates suggest the presence of defect trap states at $E_c - E_t = 0.2$ eV below the conduction band. We attribute these trap states to defects in the grain boundaries. Combining these diverse experimental results on the electronic structure of $BiFeO_3$, we propose the schematic energy-band diagram for $BiFeO_3$ ceramics shown in Fig. 4. From this schematic, it can be observed that the electrical-transport properties are dominated by the presence of shallow-trapping states $\sim$0.2 eV below the conduction band and the Fermi energy falls midway between the valence and conduction bands. Based on these results, we suggest that the intrinsic band gap in $BiFeO_3$ ceramics is $\sim$2.5 eV but that the optical spectrum may be sensitive to vacancy defects.

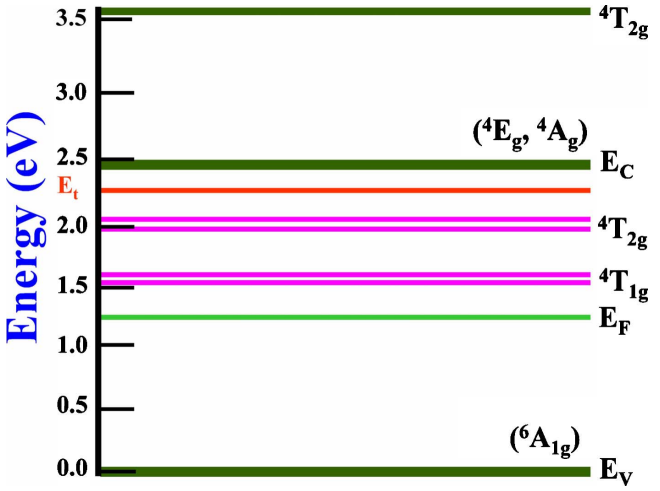

FIG. 4. (Color online) Schematic electronic energy-level diagram of polycrystalline $BiFeO_3$. E_V—valence band, E_C—conduction band, E_F—Fermi energy level, E_t—trap states, and $^6A_{1g}\rightarrow{}^4T_{2g}$ and $^6A_{1g}\rightarrow{}^4T_{1g}$—$d$-$d$ transitions of Fe^{3+} ion.

We have studied the compositional, optical, and current-density-electric field (J-E) characteristic properties of $BiFeO_3$ ceramics. X-ray photoelectron spectroscopy studies confirm a single-phase $BiFeO_3$ ceramic with evidence only for Fe^{3+} valence states with no Fe^{2+} impurities in the sample. The separation between the valence-band energy (E_V) and the Fermi energy (E_F) was found to be $\sim$1.25 eV from measurements of the binding energy of the valence band of $BiFeO_3$ ceramics. Diffuse reflectance spectra were recorded using a dilution method by mixing 10 wt % of $BiFeO_3$ powder with an inactive and nonabsorbing standard $BaSO_4$ powder. The Kubelka-Munk function, $F(R)$, was plotted and direct band gap of the sample was found to be $\sim$2.5 eV by extrapolating the relation $F(R)^{1/2}$ to zero. The near band-gap charge-transfer bands and d-d transitions of Fe^{3+} ions were also calculated from the deconvoluted DRS spectrum. Two strong transitions near 3.6 and 4.8 eV are assigned as CT excitations. Two doubly degenerated d-d transitions ($^6A_{1g}\rightarrow{}^4T_{2g}$ and $^6A_{1g}\rightarrow{}^4T_{1g}$) were observed in the energy range from 1 to 2.5 eV. The J-E characteristics of $BiFeO_3$ ceramics followed trap-filled space-charge-limited conduction mechanism above the applied voltage of 1.92 kV and trap level was found at 0.2 eV below the conduction band. Finally, an energy-band diagram of $BiFeO_3$ ceramics has been proposed based on the experimental results.

The authors acknowledge support from the Jane and Frank Warchol Foundation for their financial support for the Indo-U.S. exchange program. The author M.S.R.R. acknowledges support from Department of Science & Technology, India (Project No. SR/CMP-23/2005). G.L. acknowledges support from the National Science Foundation through Grant No. DMR-0644823.

*Corresponding author; msrrao@iitm.ac.in

[1] M. Fiebig, J. Phys. D **38**, R123 (2005).
[2] W. Eerenstein, N. D. Mathur, and J. F. Scott, Nature (London) **442**, 759 (2006).
[3] A. B. Harris, Phys. Rev. B **76**, 054447 (2007).
[4] S. R. Basu, L. W. Martin, Y. H. Chu, M. Gajek, R. Ramesh, R. C. Rai, X. Xu, and J. L. Musfeldt, Appl. Phys. Lett. **92**, 091905 (2008).
[5] A. G. Gavriliuk, V. V. Struzhkin, I. S. Lyubutin, S. G. Ovchinnikov, M. Y. Hu, and P. Chow, Phys. Rev. B **77**, 155112 (2008).
[6] R. Palai, R. S. Katiyar, H. Schmid, P. Tissot, S. J. Clark, J. Robertson, S. A. T. Redfern, G. Catalan, and J. F. Scott, Phys. Rev. B **77**, 014110 (2008).
[7] T. Kanai, S. Ohkoshi, and K. Hashimoto, J. Phys. Chem. Solids **64**, 391 (2003).
[8] A. Kumar, R. C. Rai, N. J. Podraza, S. Denev, N. Ramirez, Y. H. Chu, L. W. Martin, J. Ihlefeld, T. Heeg, J. Schubert, D. G. Schlom, J. Orenstein, R. Ramesh, R. W. Collins, J. L. Musfeldt, and V. Gopalan, Appl. Phys. Lett. **92**, 121915 (2008).
[9] R. V. Pisarev, A. S. Moskvin, A. M. Kalashnikova, and Th. Rasing, Phys. Rev. B **79**, 235128 (2009).
[10] V. Fruth, E. Tenea, M. Gartner, M. Anastasescu, D. Berger, R. Ramer, and M. Zaharescu, J. Eur. Ceram. Soc. **27**, 937 (2007).
[11] A. Pimenov, A. A. Mukhin, V. Y. Ivanov, V. D. Travkin, A. M. Balbashov, and A. Loidl, Nat. Phys. **2**, 97 (2006).
[12] R. L. Greene, D. D. Sell, W. M. Yen, and A. L. Schawlow, Phys. Rev. Lett. **15**, 656 (1965).
[13] B. Ramachandran and M. S. Ramachandra Rao, Appl. Phys. Lett. **95**, 142505 (2009).
[14] G. Kortüm, *Reflectance Spectroscopy: Principles, Methods, Applications* (Springer, New York, 1969), p. 111.
[15] X. Qi, J. Dho, R. Tomov, M. G. Blamire, and J. L. M. Driscoll, Appl. Phys. Lett. **86**, 062903 (2005).
[16] S. J. Clark and J. Robertson, Appl. Phys. Lett. **90**, 132903 (2007).
[17] J. B. Neaton, C. Ederer, U. V. Waghmare, N. A. Spaldin, and K. M. Rabe, Phys. Rev. B **71**, 014113 (2005).
[18] X. S. Xu, T. V. Brinzari, S. Lee, Y. H. Chu, L. W. Martin, A. Kumar, S. McGill, R. C. Rai, R. Ramesh, V. Gopalan, S. W. Cheong, and J. L. Musfeldt, Phys. Rev. B **79**, 134425 (2009).
[19] M. O. Ramirez, A. Kumar, S. A. Denev, N. J. Podraza, X. S. Xu, R. C. Rai, Y. H. Chu, J. Seidel, L. W. Martin, S.-Y. Yang, E. Saiz, J. F. Ihlefeld, S. Lee, J. Klug, S. W. Cheong, M. J. Bedzyk, O. Auciello, D. G. Schlom, R. Ramesh, J. Orenstein, J. L. Musfeldt, and V. Gopalan, Phys. Rev. B **79**, 224106 (2009).
[20] S.-T. Chang and J. Y.-M. Lee, Appl. Phys. Lett. **80**, 655 (2002).